

Phylogenetic Relationships and Taxonomic Position of the Ribbon Worms of the Genus *Parahubrechtia* (Nemertea, Palaeonemertea) with Descriptions of Two New Species

Alexei V. Chernyshev^{1,*}, Neonila E. Polyakova¹, and Shi-Chun Sun²

¹A.V. Zhirmunsky National Scientific Center of Marine Biology, Far Eastern Branch, Russian Academy of Sciences, Palchevskogo Street 17, Vladivostok 690041, Russia. *Correspondence: E-mail: nemertea1969@gmail.com (Chernyshev). E-mail: nila.polyakova@gmail.com (Polyakova)

²Institute of Evolution & Marine Biodiversity, Ocean University of China, 5 Yushan Road, Qingdao 266003, China. E-mail: sunsc@ouc.edu.cn (Sun)

Received 1 May 2021 / Accepted 13 May 2022 / Published 15 August 2022
Communicated by Benny K.K. Chan

The genus *Parahubrechtia* Gibson and Sundberg, 1999 was first described within the family Hubrechtidae (class Pilidiophora) and subsequently transferred to the family Callineridae (class Palaeonemertea). Here we describe two new species, *Parahubrechtia rayi* sp. nov. from the Sea of Japan (Russia) and *P. peri* sp. nov. from the South China Sea (China). A phylogenetic analysis based on partial sequences of five nuclear and mitochondrial gene regions, 18S rRNA, 28S rRNA, histone H3, 16S rRNA, and *COI*, has confirmed the monophyly of the genus *Parahubrechtia*, and indicated a close relationship to *Callinera* Bergendal, 1900, whose monophyly is not confirmed. Both genera belong to the family Tubulanidae, with its junior synonym being Callineridae. Three major subclades are distinguished within the Tubulanidae: subclade *Tubulanus* s. str., subclade *Tubulanus punctatus*, and subclade *Parahubrechtia* + *Callinera*. The further status of *Parahubrechtia* depends on whether the paraphyly of *Callinera* is confirmed or not and how the problem of paraphyly of the genus *Tubulanus* Renier, 1804 is resolved.

Key words: Nemerteans, *Callinera*, Tubulanidae, cLSM, Phylogenetic analysis, Larva.

BACKGROUND

Nemerteans, or ribbon worms, are mostly marine, unsegmented, vermiform spiralians characterized by the unique, eversible proboscis located in a coelom-like chamber referred to as rhynchocoel. The phylum Nemertea, comprised of about 1340 species (Gibson 1995; Kajihara et al. 2008; Chernyshev 2021), is currently divided into three classes, Palaeonemertea, Pilidiophora, and Hoplonemertea (Strand et al. 2019). All pilidioporans and most hoplonemerteans have a pair of sensory cerebral organs connected with the brain. Among palaeonemerteans, the cerebral organs are absent in all species of the families Carinomidae

Bürger, 1892, Cephalotrichidae McIntosh, 1873–1874, and Cephalotrichellidae Chernyshev, 2011, whereas in the family Tubulanidae Bürger, 1904 these organs are found only in the genus *Tubulanus* Renier, 1804. *Parahubrechtia* Gibson and Sundberg, 1999 is a tubulanid genus whose members lack the cerebral organs but have the epidermal lateral organs. These two traits are characteristic of species of the other two palaeonemertean genera, *Callinera* Bergendal, 1900 and *Carinomella* Coe, 1905, but both genera were originally attributed to palaeonemerteans, whereas *Parahubrechtia* was described as a genus of the family Hubrechtidae Bürger, 1892 (Gibson and Sundberg 1999) from the class Pilidiophora (Thollessen and Norenburg 2003).

The reason was a cladistic analysis based on 50 characters, which showed that the yet undescribed species HK sp.2 (= *Parahubrechtia jillae* Gibson and Sundberg, 1999) was a sister clade to the genera *Hubrechtella* Bergendal, 1902 and *Tetramys* Iwata, 1957, and *Tubulanus lucidus* Iwata, 1952 (Sundberg and Hylbom 1994). If the morphology of *T. lucidus* indicates that it belongs to the genus *Hubrechtella*, then *P. jillae* is more similar, in some characters, to palaeonemertean of the genera *Callinera* and *Carinesta* Punnett, 1900 (Chernyshev 2002), which allowed placing the *Parahubrechtia* in the family Callineridae subsequently (Chernyshev 2011; Norenburg et al. 2022). A molecular phylogenetic analysis has confirmed that two species of *Parahubrechtia*, *P. kvisti* Chernyshev, 2016 and *Parahubrechtia* sp., are indeed closely related to *Callinera* (Kvist et al. 2015; Chernyshev and Polyakova 2019; Hookabe et al. 2020), but the status of both genera has not been discussed. In the present report, we describe two new species of *Parahubrechtia* and discuss the phylogenetic position of this genus within the Palaeonemertea on the basis of partial sequences of five nuclear and mitochondrial gene regions (*18S* rRNA, *28S* rRNA, histone 3, *16S* rRNA, and cytochrome *c* oxidase subunit I). Also, we address some taxonomic issues related to the family Tubulanidae, the largest and taxonomically most complex family in the class Palaeonemertea.

MATERIALS AND METHODS

Specimen collection and morphological observation

Samples were collected from two localities: Peter the Great Bay, Sea of Japan (Russia) and Beihai, Guanxi Province, South China Sea (China) (see below for detailed collecting information). Live specimens of *Parahubrechtia rayi* sp. nov. were collected by dredge from depths 3–4 m and examined under a stereo microscope (Leica MZ 12.5) equipped with a camera (Leica DFC 290). Adults of *Parahubrechtia peri* sp. nov. were collected by digging muddy sand at the intertidal zone. Live specimens of *P. peri* sp. nov. were examined and photographed under a stereo microscope (Nikon SMZ800) equipped with a camera (Nikon DSL1) or a microscope (Nikon E600) equipped with a camera (Olympus DP72). Specimens for histological studies were anaesthetised in a $MgCl_2$ solution isotonic to seawater, fixed in Bouin's fluid or 10% formalin for 72 h, and transferred to 70% EtOH through an ethanol series of increasing concentrations. Molecular materials (complete worms or the posterior region of

some worms) were preserved in 95% ethanol, and kept at $-20^{\circ}C$ until DNA extraction. Serial paraffin sections 5–6 μm thick were stained by the Mallory's trichrome method. The sections were photographed with an AxioCam Icc1 digital camera attached to a Zeiss Discovery V12 stereomicroscope, or with an AxioCam HR3 digital camera attached to a Zeiss Imager Z2 compound microscope. For confocal laser scanning microscopy (cLSM) studies, pieces of body and proboscis of *P. ray* sp. nov. were fixed for 4 h at room temperature (RT) with a 4% paraformaldehyde solution in phosphate-buffered saline (PBS), rinsed thrice in PBS (0.1 M), and stained for 2–8 h at RT with phalloidin-Alexa Fluor 633 (Invitrogen) at 1 U per 100 mL of 1% Triton X-100 in PBS with 1 mg mL⁻¹ DAPI (Invitrogen). To examine the serotonergic nervous system, pieces of the body tissues were transferred to a solution of antiserotonin primary antibody (5-HT, polyclonal, rabbit, diluted 1 : 2000, Immunostar, USA) in PBS with 1% bovine serum albumin (BSA, Immunostar, USA). The pieces were washed in PBS, immersed in Mowiol 4–88 (Aldrich), and mounted on glass slides. The specimens were examined under a LSM-780 confocal microscope (Carl Zeiss, Germany). The obtained image series was analyzed using the CLSM-780 software. Type specimens are deposited at the Museum of the A. V. Zhirmunsky National Scientific Center of Marine Biology FEB RAS, Vladivostok, Russia (MIMB) (see species descriptions). Abbreviations for descriptions are as follows: E, epidermis; D, dermis; DM, diagonal musculature; ICM, inner circular musculature; LM, longitudinal musculature; OCM, outer circular musculature.

DNA extraction, PCR amplification, and sequencing

The new sequences (Table 1), except sequences of *P. peri*, were obtained at the Laboratory of Genetics, A.V. Zhirmunsky National Scientific Center of Marine Biology FEB RAS. Total genomic DNA was extracted from the ethanol-preserved specimens using the DNA-sorb-B-100 Blood Kit (CMD) and DNeasy Blood & Tissue Kit (Qiagen) according to the manufacturer's protocol. Five markers of partial nuclear *18S* rRNA, *28S* rRNA, histone *H3*, mitochondrial *16S* rRNA and cytochrome *c* oxidase subunit I (*COI*) sequences were amplified from the genomic DNA. Polymerase chain reaction (PCR) was carried out using the primers listed in table 1. PCR cycling profiles were as follows: *COI* – 2 min at $95^{\circ}C$, followed by 40 cycles of 40 s at $95^{\circ}C$, 40 s at $50^{\circ}C$, and 1 min at $72^{\circ}C$, and finally 7 min at $72^{\circ}C$; *16S* – 2 min at $94^{\circ}C$, 35 cycles with 40 s at $94^{\circ}C$, 40 s at $48^{\circ}C$, and 1 min at $72^{\circ}C$, and finally 7 min at

72°C; *18S* – 2 min at 94°C, 40 cycles with 1 min at 94°C, 1 min at 52°C, and 1 min at 72°C, and finally 7 min at 72°C (for primer pairs Tim A – 1100R and 3F-18Sbi), and 50°C (for primer pair 18Sa2.0 – 9R); *28S* – 2 min at 94°C, 40 cycles with 40 s at 94°C, 40 s at 52°C, and 1 min at 72°C, and finally 7 min at 72°C; Histone *H3* – 2 min at 94°C, 35 cycles of 40 s at 94°C, 40 s at 55°C, and 1 min at 72°C, and finally 7 min at 72°C. The amplified products were purified using ExoSAP (Fermentas, Lithuania). Sequencing in forward and reverse directions was carried out on an ABI Prism 3500 Genetic Analyzer (Applied Biosystems) under conditions recommended by the manufacturer, using a BigDye Terminator Cycle Sequencing Kit (ver. 3.1, Applied Biosystems, Foster City, CA, USA) and the same primers as for PCR.

The sequences for *P. peri* were obtained at the Institute of Evolution and Marine Biodiversity, Ocean University of China. Total genomic DNA was extracted from the ethanol-preserved specimens using the MicroElute Genomic DNA Kit (Omega) according to the manufacturer’s protocol. PCR primers for *18S* were EukF and SR7, those for *COI*, *16S* and *28S* were the same as aforementioned (Table 1). PCR cycling profiles were as follows: *COI* – 5 min at 94°C, followed by 35 cycles of 30 s at 94°C, 30 s at 52°C, and 1 min at 72°C, and finally 3 min at 72°C; *16S* – 5 min at 94°C, 35 cycles with 30 s at 94°C, 30 s at 48°C, and 1 min at 72°C, and finally 3 min at 72°C; *18S* – 5 min at 94°C, 35 cycles with 30 s at 94°C, 30 s at 52°C, and 1 min at 72°C, and finally 3 min at 72°C; Histone *H3* – 5 min at 94°C, 35 cycles of 30 s at 94°C, 30 s at 55°C, and 1 min at 72°C, and finally 3 min at 72°C. Purification

and sequencing (forward and reverse directions using the same primers as for PCR) were carried out at BGI (Shenzhen, China).

All the new sequences were submitted to GenBank (accession numbers are listed in the Table 2). The sequences for all five markers were aligned using MAFFT ver. 7 (Kato and Standley 2013) with default parameters. Ambiguous positions and gaps were discarded from the subsequent analysis using GBlocks (Castresana 2000), which resulted in a final dataset of *16S* (453 bp), *18S* (1699 bp), *28S* (499 bp), *COI* (657 bp), and *H3* (329 bp). A supermatrix was formed by concatenating the five markers (*16S*, *COI*, *18S*, *28S*, and histone *H3*) using SequenceMatrix (Vaidya et al. 2011), wherein the external gaps were coded as ‘missing data’ (Table 3).

The simultaneous selection of the partition schemes, as well as the search for the optimal nucleotide substitution models for the supermatrix were carried out using PartitionFinder (Lanfear et al. 2012 2014) with implementation of the ‘greedy’ search scheme. Accordingly, the final supermatrix was divided into seven character sets (Table 3). The newly generated dataset (five species from three families) was combined with previously published partial sequences of *16S*, *18S*, *28S*, *COI*, and *H3* for 31–33 nemertean species from 10–11 families. Six out-group species of the genera *Cephalothrix* Oersted, 1843, *Cephalotrichella* Wijnhoff, 1913, and *Balionemertes* Sundberg, Gibson and Olson, 2003 were included in the phylogenetic analysis. A combined analysis based on the five concatenated genes was conducted using Bayesian inference (BI) and maximum likelihood (ML) analyses. BI analyses

Table 1. List of primers used in the present study. Forward primer sequences are denoted in bold font

Target locus	Primer name	Primer sequence 5’–3’	References
<i>16S</i> RNA	ar-L	CGCCTGTTTATCAAAAACAT	Palumbi et al. 1991
	br-H	CCGGTCTGAACTCAGATCACGT	Palumbi et al. 1991
<i>COI</i>	LCO1490	GGTCAACAAAATCATAAAGATATGG	Folmer et al. 1994
	HCO2198	TAAACTTCAGGGTGACCAAAAATCA	Folmer et al. 1994
<i>28S</i> RNA	LSU5	ACCCGCTGAATTTAAGCAT	Littlewood 1994
	LSU3	TCCTGAGGGAAACTTCGG	Littlewood 1994
	Tim A	AMCTGGTTGATCCTGCCAG	Noren and Jondelius 1999
	1100R	GATCGTCTTCGAACCTCTG	Noren and Jondelius 1999
	3F	GTTCGATTCGGGAGAGGGA	Giribet et al. 1996
<i>18S</i> RNA	18Sbi	GAGTCTCGTTTCGTTATCGGA	Whiting et al. 1997
	18Sa2.0	ATGGTTGCAAAGCTGAAAC	Whiting et al. 1997
	9R	GATCCTTCGGCAGGTTACCTAC	Giribet et al. 1996
	EukF	AACCTGGTTGATCCTGCCAGT	Sands et al. 2008
	SR7	GTTCAACTACGAGCTTTTTAA	Vilgalys and Sun 1994
<i>H3</i>	aF	ATGGCTCGTACCAAGCAGAC	Colgan et al. 1998
	aR	ATATCCTTRGGCATTRATRGTGAC	Colgan et al. 1998

Table 2. List of species included in the phylogenetic analysis with GenBank accession numbers for sequences (sequences new to this study in bold)

Species	Locality	16S	18S
<i>Callinera grandis</i>	Sweden, Skagerak	JF277570	JF293067
<i>Callinera kasyanovi</i>	Russia, PGB, SJ	KP270840	KP270790
<i>Callinera</i> sp. 7 Vostok	Russia, PGB, SJ	-	MZ744957
<i>Callinera</i> sp. 17 Alaska	USA, AK	MZ744983	MZ744958
<i>Callinera</i> sp. IZ 45635	Russia, PGB, SJ	KP270839	KP270789
<i>Carinina plecta</i>	Japan	-	EU495307
<i>Parahubrechtia kvisti</i> IZ-45633	Vietnam, Nam Zu Is.	KP270848	KP270798
<i>Parahubrechtia</i> peri A10	China, SCS, Beihai	MZ744984	MZ744959
<i>Parahubrechtia</i> peri A15	China, SCS, Beihai	MZ744985	MZ744960
<i>Parahubrechtia</i> peri A16	China, SCS, Beihai	MZ744986	-
<i>Parahubrechtia</i> rayi	Russia, SJ, PGB, ZR	MZ744987	MZ744961
<i>Parahubrechtia</i> rayi 29 Vostok	Russia, SJ, PGB, VB	-	MZ744962
<i>Parahubrechtia rayi</i> IZ 45554 = Tubulanidae sp. IZ- 45554	Russia, SJ, PGB, VB	KP270844	KP270794
<i>Parahubrechtia rayi</i> MS 2008	Russia, SJ, PGB, VB	-	EU495309
Tubulanidae sp. 14DS	Russia, between KKT and Kuril Is.	MF512038	MF512063
Tubulanidae sp. 33DS	Russia, SO	MF512040	MF512065
Tubulanidae sp. 33Q California	USA, CA	MZ744988	MZ744963
Tubulanidae sp. IZ 45557	Abyssal plain adjacent to KKT	KP270846	KP270796
Tubulanidae sp. Kurambio2 17	Russia, KKT	MN211470	MN211371
Tubulanidae Kurambio2 77/1	Russia, KKT	MN211469	MN211369
Tubulanidae Kurambio2 77/4	Russia, KKT	-	MN211370
Tubulanidae Kurambio2 90	Russia, KKT	MN211471	MN211372
Tubulanidae Vema3	Vema Fracture Zone	-	-
Tubulanidae Vema4	Vema Fracture Zone	KY296889	MF512060
Tubulanidae Vema6	Vema Fracture Zone	KY296890	MF512061
<i>Tubulanus annulatus</i>	Sweden, Skagerak	JF277599	JF293060
<i>Tubulanus</i> cf. ezoensis	Russia, SO, Yerineyskaya Guba	MZ744989	MZ744964
<i>Tubulanus ezoensis</i>	Russia, SO, Iturup Is.	MZ744990	MZ744965
<i>Tubulanus izuensis</i>	Japan, Suruga Bay	MT809229	MT809204
<i>Tubulanus pellucidus</i>	USA, NC	JF277595	JF293062
<i>Tubulanus polymorphus</i>	USA, San Juan Is.	JF277598	JF293061
<i>Tubulanus punctatus</i>	Japan, Akkeshi Bay	JF277597	JF293063
<i>Tubulanus punctatus</i> 3 Vostok	Russia, SJ, PGB, VB	MZ744991	MZ744966
<i>Tubulanus rhabdotus</i>	USA, FL	AJ436839	-
<i>Tubulanus riceae</i>	Panama, CS	MZ744992	MZ744967
<i>Tubulanus sexlineatus</i>	USA, Seattle	JF277596	JF293064
<i>Tubulanus</i> sp. B Sakhalin	Russia, SO, Sakhalin Is. (depth 475-484 m)	MZ744993	MZ744968
<i>Tubulanus</i> sp. D Antarctica	Antarctica, Prydz Bay	MZ744994	MZ744969
<i>Tubulanus</i> sp. E Antarctica	Antarctica, Mawson cape (depth 495 m)	-	MZ744970
<i>Tubulanus</i> sp. IZ 45552	Russia, SJ, PGB, VB	KP270843	KP270793
<i>Tubulanus</i> sp. IZ 45559	Russia, SO, Iturup Is.	KP270847	KP270797
<i>Tubulanus tamias</i>	Japan, Tomioka Bay	LC042091	LC042092
<i>Balionemertes australiensis</i>	USA, Guam	-	MK309617
<i>Cephalothrix bipunctata</i>	Spain	KF935447	KF935279
<i>Cephalotrichella echinicola</i>	Vietnam	MK309618	MK309614
<i>Cephalothrix filiformis</i>	Germany	JF277593	JF293053
<i>Cephalothrix hongkongiensis</i>	China	JF277591	JF293057
<i>Cephalothrix iwatai</i> IZ 45650	Russia, SJ, Gamov Canyon	KP270850	KP270800

Table 2. (Continued)

Species	28S	COI	H3	References
<i>Callinera grandis</i>	-	HQ848626	JF277709	Andrade et al. 2012
<i>Callinera kasyanovi</i>	KP270816	KP270865	-	Kvist et al. 2015
Callinera sp. 7 Vostok	MZ744977	MZ772874	MZ772887	Present paper
Callinera sp. 17 Alaska	MZ744978	-	MZ772888	Present paper
<i>Callinera</i> sp. IZ 45635	KP270815	KP270864	-	Kvist et al. 2015
<i>Carinina plecta</i>	-	EU489493	-	Sundberg et al. 2009
<i>Parahubrechtia kvisti</i> IZ-45633	-	KP270871	-	Kvist et al. 2015
Parahubrechtia peri A10	-	MZ772875	MZ772889	Present paper
Parahubrechtia peri A15	-	MZ772876	MZ772890	Present paper
Parahubrechtia peri A16	-	MZ772877	MZ772891	Present paper
Parahubrechtia rayi	-	MZ772878	MZ772892	Present paper
Parahubrechtia rayi 29 Vostok	-	MZ772879	MZ772893	Present paper
<i>Parahubrechtia rayi</i> IZ 45554 = Tubulanidae sp. IZ- 45554	KP270820	KP270869	MN205445*	Kvist et al. 2015; *Chernyshev and Polyakova 2019
<i>Parahubrechtia rayi</i> MS 2008	-	EU489499	-	Sundberg et al. 2009
Tubulanidae sp.14DS	MF512089	MF512113	MF512132	Chernyshev and Polyakova 2018a
Tubulanidae sp. 33DS	MF512091	MF512115	MF512133	Chernyshev and Polyakova 2018a
Tubulanidae sp. 33Q California	MZ744979	-	MZ772894	Present paper
Tubulanidae sp. IZ 45557	KP270822	-	-	Kvist et al. 2015
Tubulanidae sp. Kurambio2 17	MN211424	MN205495	MN205443	Chernyshev and Polyakova 2019
Tubulanidae Kurambio2 77/1	MN211422	MN205494	MN205442	Chernyshev and Polyakova 2019
Tubulanidae Kurambio2 77/4	MN211423	-	MN205443	Chernyshev and Polyakova 2019
Tubulanidae Kurambio2 90	MN211425	-	MN205446	Chernyshev and Polyakova 2019
Tubulanidae Vema3	KY296899	KY296908	KY296917	Chernyshev and Polyakova 2018b
Tubulanidae Vema4	KY296900	KY296909	KY296918	Chernyshev and Polyakova 2018b
Tubulanidae Vema6	KY296902	KY296911	KY296920	Chernyshev and Polyakova 2018b
<i>Tubulanus annulatus</i>	HQ856901	HQ848622	JF277717	Andrade et al. 2012
Tubulanus cf. ezoensis	-	MZ772880	MZ772895	Present paper
Tubulanus ezoensis	MZ744980	MZ772881	MZ772896	Present paper
<i>Tubulanus izuensis</i>	-	MT811763	LC581475	Hookabe et al., 2020
<i>Tubulanus pellucidus</i>	HQ856900	HQ848625	JF277708	Andrade et al. 2012
<i>Tubulanus polymorphus</i>	HQ856899	HQ848621	JF277716	Andrade et al. 2012
<i>Tubulanus punctatus</i>	HQ856894	HQ848624	JF277748	Andrade et al. 2012
Tubulanus punctatus 3 Vostok	-	MZ772882	MZ772897	Present paper
<i>Tubulanus rhabdotus</i>	AJ436894	AJ436948	AJ436990	Tholleson and Norenburg 2003
Tubulanus riceae	-	MZ772883	MZ772898	Present paper
<i>Tubulanus sexlineatus</i>	HQ856895	JF277747	HQ848623	Andrade et al. 2012
Tubulanus sp. B Sakhalin	-	MZ772884	MZ772899	Present paper
Tubulanus sp. D Antarctica	MZ744981	MZ772885	MZ772900	Present paper
Tubulanus sp. E Antarctica	MZ744982	MZ772886	MZ772901	Present paper
<i>Tubulanus</i> sp. IZ 45552	KP270819	KP270868	MZ772902*	Kvist et al. 2015; *Present paper
<i>Tubulanus</i> sp. IZ 45559	KP270823	KP270870	-	Kvist et al. 2015
<i>Tubulanus tamias</i>	AB854624	LC042093	LC042094	Kajihara et al. 2015
<i>Balionemertes australiensis</i>	MK309624	MK307892	MK309328	Chernyshev et al. 2019
<i>Cephalothrix bipunctata</i>	KF935335	KF935501	KF935391	Kvist et al. 2014
<i>Cephalothrixella echinicola</i>	MK309621	MK307889	MK309325	Chernyshev et al. 2019
<i>Cephalothrix filiformis</i>	HQ856843	HQ848617	JF277742	Andrade et al. 2012
<i>Cephalothrix hongkongiensis</i>	HQ856839	HQ848614	JF277739	Andrade et al. 2012
<i>Cephalothrix iwatai</i> IZ 45650	KP270825	KP270873	MW328562	Kvist et al. 2015

Abbreviations: CS, Caribbean Sea; KKT, Kuril-Kamchatka Trench; PGB, Peter the Great Bay; SCS, South China Sea; SJ, Sea of Japan; SO, Sea of Okhotsk; VB, Vostok Bay; ZR, Zolotoy Rog Bay.

were carried out in MrBayes (ver. 3.2, see <http://www.mrbayes.net/>; Ronquist et al. 2012), launching two parallel runs with four Markov chains in each run (three cold and one hot) during 2,500,000 generations. The values of run convergence indicated that a sufficient number of trees and parameters were sampled (Table 3). Based on the convergence of likelihood scores, 25% of sampled trees were discarded as burn-in. The rest was used to build the consensus tree while the nodes with posterior probabilities less than 0.5 were collapsed. The maximum-likelihood phylogenetic tree was inferred using the edge-linked partition model on the IQ-TREE web server (Nguyen et al. 2015); branch supports with the 1,000 ultrafast bootstrap replicates were obtained in the IQ-TREE software (Minh et al. 2013).

RESULTS

SYSTEMATICS

Class Palaeonemertea Hubrecht, 1879
Family Tubulanidae Bürger, 1904
Genus *Parahubrechtia* Gibson and Sundberg, 1999

Diagnosis (modified from Gibson and Sundberg 1999): Body encircled with thin transverse ‘tubulanid ring’, lateral organs present. Body wall musculature composed of outer circular, diagonal, longitudinal, and inner circular layers. Rhynchocoel without muscle sac; rhynchocoel wall with two muscle layers, but inner longitudinal musculature can be reduced. Proboscis with outer circular, diagonal, longitudinal and inner (endothelial) circular muscle layers; two proboscis nerves present; special armament in middle region absent; pseudocnidae present. Cerebral sensory organs absent. Brain and lateral nerve cords located between epidermal basement membrane and body wall outer circular muscles; nervous system lacks neurochords

and neurochord cells; buccal nerves paired; cephalic region with subepidermal nerve layer but without rhynchodaeum nerves. Frontal glands and apical organ absent. Intestine without lateral diverticula. Blood vascular system simple, without mid-dorsal and rhynchocoel vessels; pair of cephalic lacunae present; lateral vessels run internal to ICM in foregut region and external to ICM in intestine region. Excretory system simple, anteriorly penetrating lateral blood vessels. Dioecious.

Remarks: All species of the genus *Parahubrechtia*, including the two described in this report, have a very similar internal structure. Although no sequences have been obtained for the type species, *P. jillae*, we have no doubt that this species, *P. kvisti* Chernyshev, 2016, *P. rayi* sp. nov., and *P. peri* sp. nov. belong to a single genus. *P. jillae* and *P. kvisti* show particularly high similarity in their internal morphology.

***Parahubrechtia rayi* sp. nov.**

(Figs. 1–5)

urn:lsid:zoobank.org:act:AA3E9B9D-CCC5-482E-ADBB-1D35E6B9E7AE

Syn.: *Parahubrechtia* sp. IZ-45554 – Kvist et al. 2015; *Parahubrechtia* sp. – Chernyshev 2015; Magarlamov et al. 2021; Yurchenko et al. 2021.

Material examined: Holotype (MIMB 41337), 3 August, 2009, Sea of Japan, Peter the Great Bay, Vostok Bay (42°54'36"N, 132°43'42"E), depth 5–6 m, mud, collected by A.V. Chernyshev; paratype (MIMB 41338), collected along with holotype; paratype (MIMB 41339), 22 September, 2000, Sea of Japan, Peter the Great Bay, Vostok Bay, depth 4–5 m, mud, collected by A.V. Chernyshev; paratype (MIMB 41340), 26 July, 2020, Sea of Japan, Peter the Great Bay, Vostok Bay, depth 5–6 m, mud, collected by A.V. Chernyshev.

Other material examined: 10 specimens (MIMB), collected in Vostok Bay and Zolotoy Rog Bay of Peter the Great Bay.

Table 3. The main parameters of model-based inferred phylogeny

	Data set	Charset	Optimal model	ASD ^a	Harmonic mean	min ESS ^b	PSRF ^c
Supermatrix	charset 1	16S	GTR+I+G	0.004360	-33229.36	1053.21	1.000
	charset 2	18S	GTR+I+G				
	charset 3	28S, H3_1 ^d	GTR+I+G				
	charset 4	COI_1 ^d	GTR+I+G				
	charset 5	COI_2d, H3_2 ^d	GTR+I+G				
	charset 6	COI_3 ^d	GTR+G				
	charset 7	H3_3 ^d	GTR+I+G				

^aAverage standard deviation of split frequencies. ^bEstimated Sample Size. ^cPotential Scale Reduction Factor. ^dCodon position.

Description: External morphology of live specimens: Live worms 10–40 mm long and 0.5–1 mm wide. Body cylindrical in foregut region, slightly flattened in posterior half. Head rounded, slightly wider than neck, but narrower than the following body region (Fig. 1A, D), flattened dorso-ventrally, with rhynchodaemum visible through integument. Mouth small, elongated (rounded when open). Cephalic furrows and ocelli absent. Body whitish in colour, partly translucent in gut region, so that gonads and gut visible through body wall (Fig. 1B, C). In nephridial region, body encircled with thin transverse epidermal ring ('tubulanid ring') (Fig. 1B); posteriorly to ring, epidermis opaque (Fig. 1B) due to large number of glands; pair of oval lateral organs located in area of epidermis opaque. Mature testes white; ovary pale pink or pale yellowish. Posterior 1/3 of body with irregularly spaced epidermal constrictions (Fig. 1B, C).

Internal morphology: Body wall in foregut region: E 61–79 μm (up to 85–120 μm in precerebral region), D 1.5–2 μm , OCM 3–6 μm , LM 30–74 μm , ICM 4–7 μm (up to 15 μm in nephridial region); crisscrossed DM between OCM and LM present in cephalic and foregut regions (Fig. 2A). ICM not visible in transverse sections through the posterior half of body, but a very thin layer of ICM detected by cLSM (Fig. 2C, F). Longitudinal muscle plate between rhynchocoel and foregut present. Two muscle crosses (dorsal and ventral) present between body OCM and ICM: dorsal cross well-developed (Figs. 2D, E; 3G, H); ventral cross thinner and not detected in gut region. Well-developed rhynchodaeal glandular epithelium forms

four folds (Fig. 3A, B). Rhynchocoel as long as half of body length; rhynchocoel wall consists of outer circular and inner longitudinal muscle layers, but longitudinal muscles reduced posterior to nephridial region (Fig. 2E, F); in some areas, inner longitudinal muscles scattered (Fig. 2D); posteriorly to nephridial region, rhynchocoel contains short inner tube with proboscis running inside (Fig. 3G); in posterior part, this tube connected first to dorsal wall of rhynchocoel (Fig. 3H), then with ventral wall. Anterior proboscis portion consists of four regions (Fig. 4A): (1) anteriorly located short muscular region without clear glandular epithelium (Fig. 4B); (2) short region with well-developed longitudinal musculature and thin epithelium with basophilic glands (Fig. 4C); (3) short region with thin musculature, wide lumen, and thick epithelium with numerous glandular cells stained with Orange G (Fig. 4D); (4) long region with typical morphology, *i.e.*, four muscular layers (endothelial circular, longitudinal, diagonal, and outer circular) and well-developed glandular epithelium (Fig. 4E). Proboscis diagonal musculature crisscrossed (Fig. 4F); two very thin muscle crosses detected by cLSM (Fig. 4G, H). Rod-shaped pseudocnidae 1.6–1.9 μm in length, located in clusters of up to 300 pseudocnidae (Magarlamov et al. 2021). Middle proboscis region with thickening of longitudinal and radial muscles (Fig. 4I). Cephalic blood lacunae voluminous in transverse sections (Fig. 3A, B). Lateral vessels run internally to ICM in foregut region (Figs. 2B; 3C), but in posterior foregut region, lateral vessels run through this layer and continue posteriorly between ICM and LM (Figs. 2C, F; 3F). Endothelium of lateral vessels with thin circular

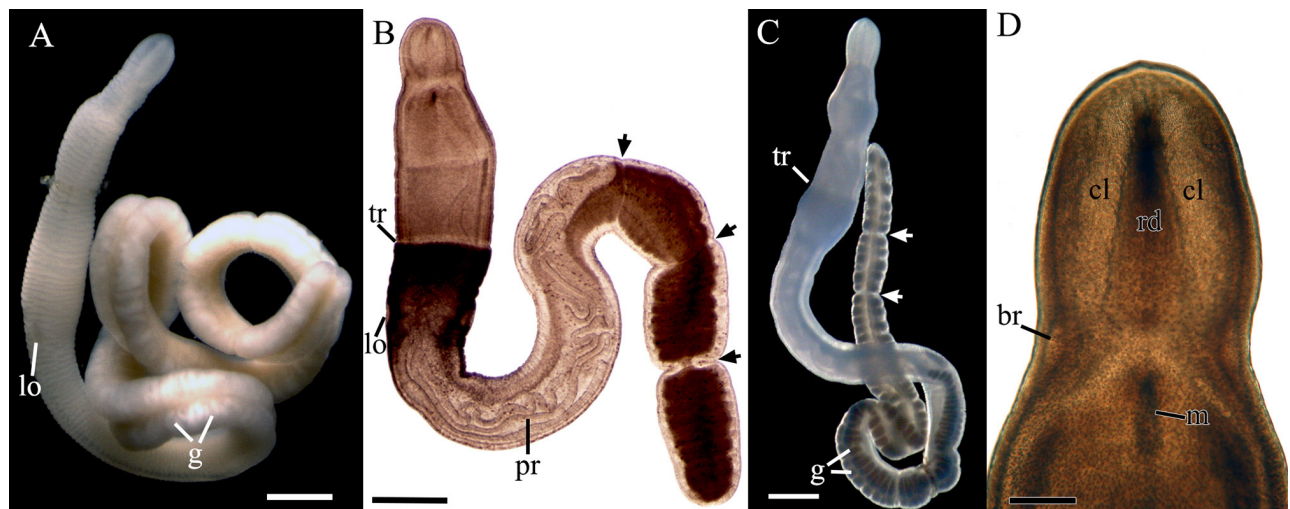


Fig. 1. *Parahubrechtia rayi* sp. nov., A, unrelaxed live holotype, mature male (MIMB 41337); B, C, specimens (B, immature male; C, mature female) compressed under coverglass (arrows indicate epidermal constrictions); D, the head of the specimen compressed under coverglass. Abbreviations: br, brain; cl, cephalic lacuna; g, gonad; lo, lateral organ; m, mouth; pr, proboscis; rd, rhynchodaemum; tr, 'tubulanid' ring. Scale bars: A–C = 0.5 mm; D = 0.1 mm.

musculature (Fig. 2C). Subepidermal nerve plexus well developed (Fig. 2G, I); transverse subepidermal nerves run/located in posterior foregut and gut region (Fig. 2G); neural plexus associated with cephalic

blood lacunae (Fig. 2H) and rhynchocoel wall (Fig. 2I). Immediately anterior to mouth, two nerves extend from ventral part of ventral brain ganglia, fuse (Fig. 3D), and split up again (Fig. 3E), forming two large

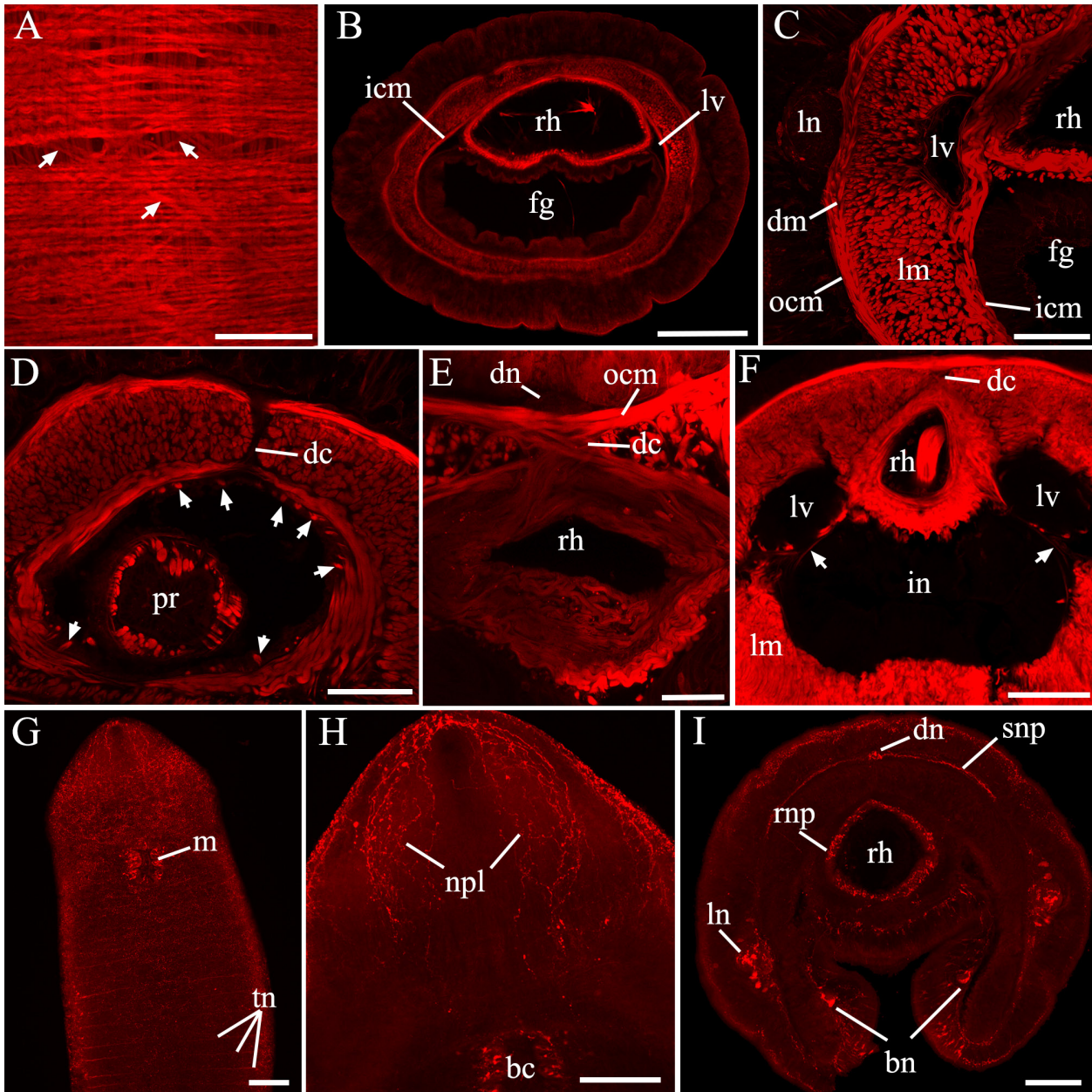


Fig. 2. *Parahubrechtia rayi* sp. nov., cLSM micrographs of the body labeled with phalloidin (A–F) and 5-HT (G–I). A, substack of longitudinal sections through the body-wall musculature with crisscrossed DM (arrowed) in the precerebral region; B, C, substacks of transverse sections through the body in the foregut region; D, substack of transverse sections through the body in the mouth region (arrows indicate isolated longitudinal muscles); E, F, substacks of transverse sections through the body in the post-nephridial region (arrows indicate ICM); G, z-projection of longitudinal sections through the anterior part of the body (ventral view) showing subepidermal neural plexus; H, substack of longitudinal sections of the anterior part of the head showing neural plexus of the cephalic lacunae; I, substack of transverse section through the body in the mouth region showing 5-HT positive nervous system. Abbreviations: bc, buccal cavity; bn, buccal nerves; dc, dorsal muscle cross; dm, diagonal musculature; dn, dorsal nerve; fg, foregut; icm, inner circular musculature; in, intestine; lm, longitudinal musculature; ln, longitudinal nerve cord; lv, lateral vessel; m, mouth; ocm, outer circular musculature; npl, neural plexus of blood lacunae; pr, proboscis; rh, rhynchocoel; rnp, rhynchocoel neural plexus; snp, subepidermal neural plexus; tn, transverse subepidermal nerves. Scale bars: A, C–E = 50 μ m; B = 200 μ m; F–H = 100 μ m; I = 20 μ m.

buccal nerves (Fig. 2I). Dorsal nerve single, upper (Fig. 2I). Nephridial tubes with pair of narrow latero-dorsal openings and terminal glandular organ protruding into blood vessels laterally (Fig. 3I). Gonadal sacs paired, opening dorsally, with first pair located immediately posterior to rhynchocoel end (Fig. 1C).

Ecology and reproduction: The species is found in habitats at depths of 4–9 m on mud and muddy sand. Development occurs in late July and in August at a water temperature of 18–20°C. Eggs are 40–45 μm in diameter, with translucent jelly coats of 185–210 μm

in diameter. At 22–26 h after external fertilization, free-swimming planula-like larvae 100–105 μm in length with long apical tuft hatched from eggs; at 1–2 days after fertilization, the length of larvae reached 120–130 μm; provisional epithelium was detected by cLSM and phalloidin labeling (Fig. 5A–C); at 24 h and 48 h post-fertilization, a pair of posterior retractor muscles are present (Fig. 5A, B); at 72 h post-fertilization, body wall musculature consists of OCM, DM, and LM (Fig. 5C). Eyes are absent. Further development was not studied.

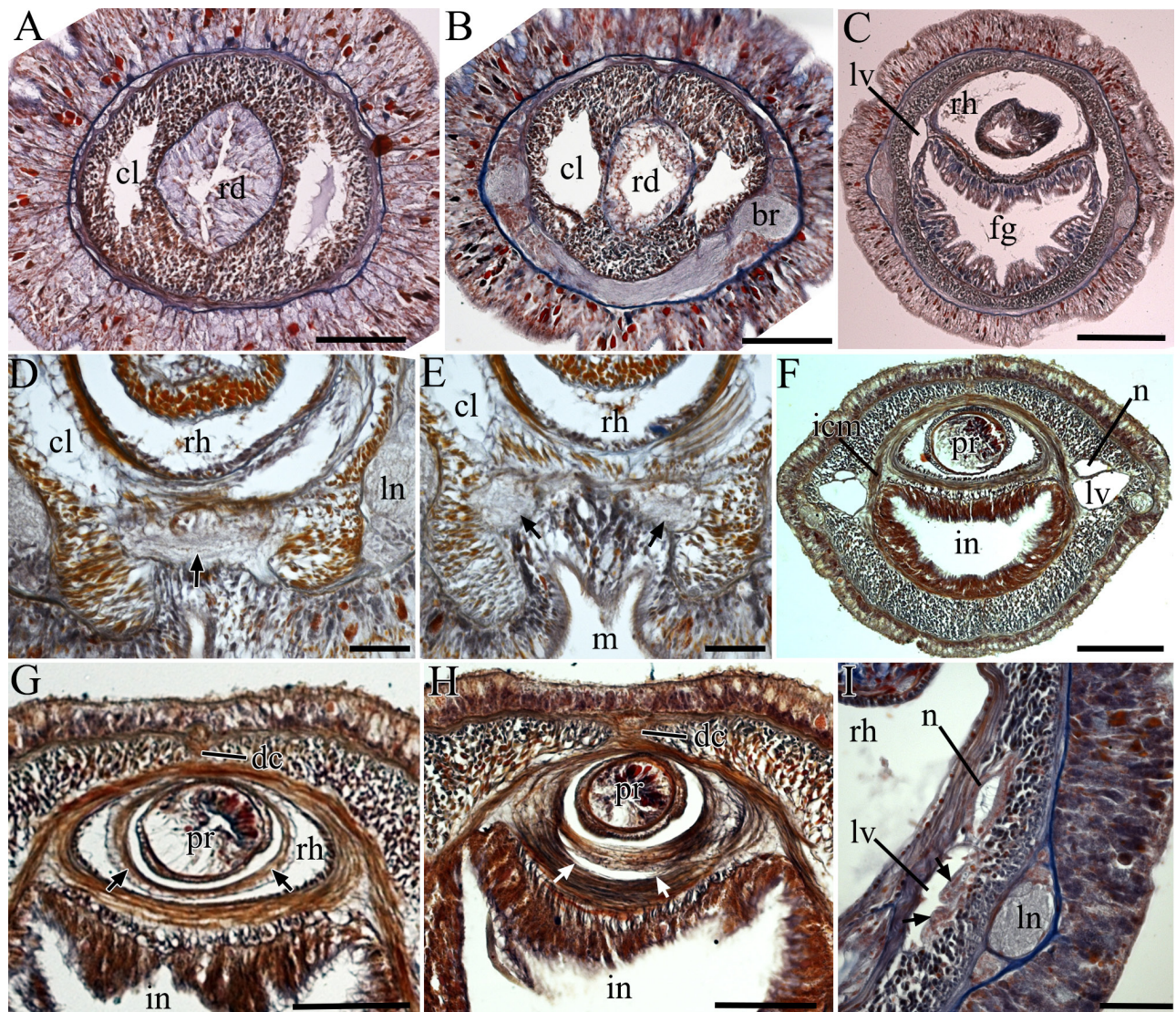


Fig. 3. *Parahubrechtia rayi* sp. nov., transverse histological sections of the holotype (F–H) and paratypes (A–E, I). A, precerebral region; B, brain region; C, foregut region; D, E, mouth region showing fused (D, arrow) and split (E, arrows) buccal nerves; F, nephridial region; G, H, post-nephridial region showing inner rhynchocoel tube (G, arrows) and ventral rhynchocoel caecum (H, arrows); I, nephridial region (arrows indicate terminal glandular organ). Abbreviations: br, brain; cl, cephalic lacuna; dc, dorsal muscle cross; fg, foregut; icm, inner circular musculature; in, intestine; ln, longitudinal nerve cord; lv, lateral vessel; m, mouth; n, nephridial tube; pr, proboscis; rd, rhynchodaem; rh, rhynchocoel. Scale bars: A, B, G, H = 100 μm; C, F = 200 μm; D, E = 50 μm.

Distribution: Sea of Japan, Peter the Great Bay (Vostok Bay and Zolotoy Rog Bay).

Etymology: The specific name honors Prof. Ray Gibson, one of the coauthors of the genus *Parahubrechtia*.

Remarks: *Parahubrechtia rayi* sp. nov. is distinguished from the two known species of *Parahubrechtia*, *P. jillae* Gibson and Sundberg, 1999 and *P. kvisti* Chernyshev, 2016, by a greater body length, the presence of two muscle crosses between body OCM and ICM, and the well-developed inner

longitudinal musculature of rhynchocoel in the foregut region. The uncorrected *p*-distances between the *COI* of the *P. rayi* and *P. kvisti* are 16.1–16.6%.

***Parahubrechtia peri* sp. nov.**

(Figs. 6, 7)

urn:lsid:zoobank.org:act:A41FA129-A0CA-4E37-B28B-71D560E7A4B4

Material examined: Holotype (MIMB 41341), 4 November 2013, South China Sea, Guanxi Province,

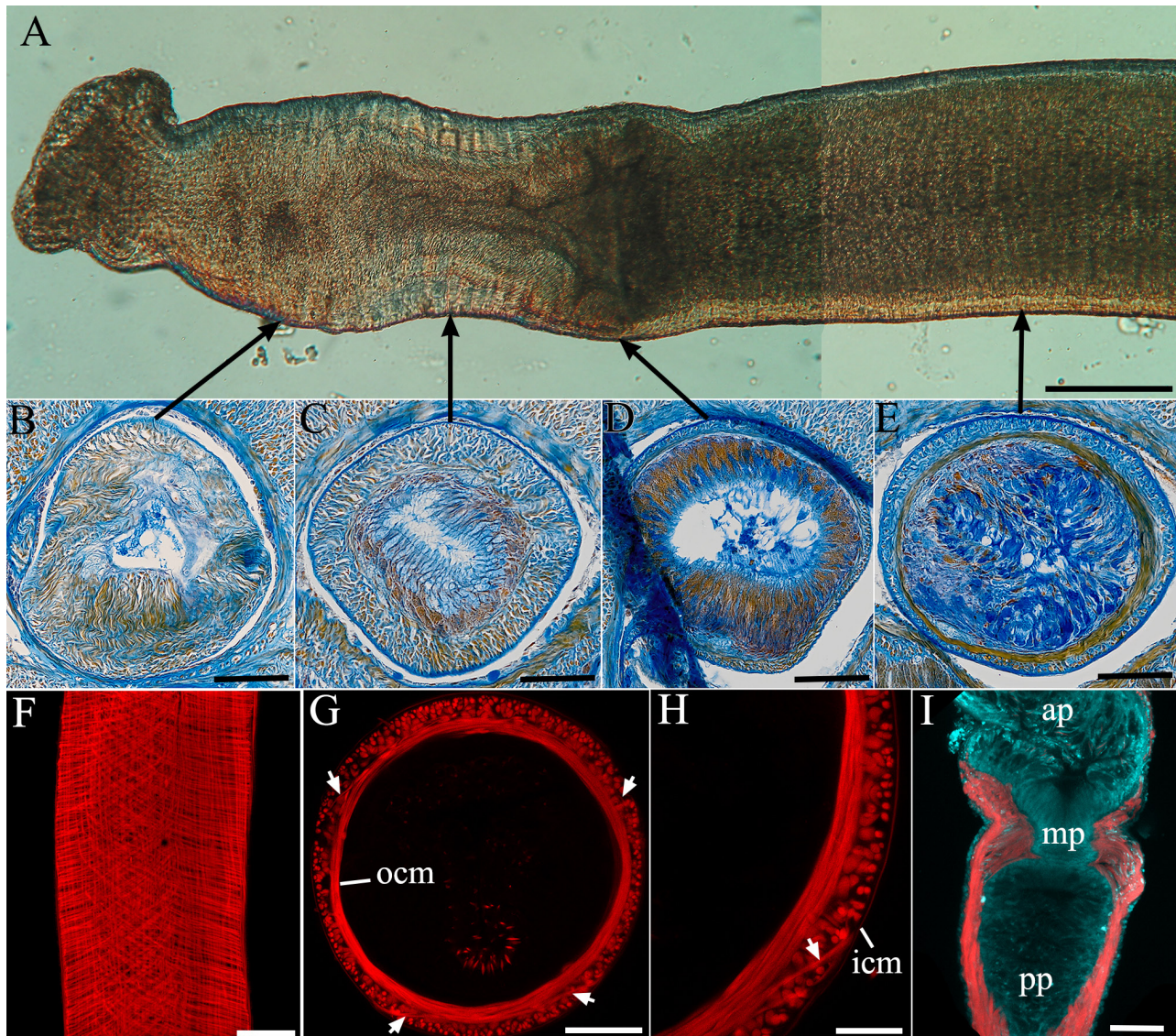


Fig. 4. *Parahubrechtia rayi* sp. nov., proboscis. A, proboscis of a live specimen compressed under coverglass (arrows indicate four proboscis regions); B–E, transverse histological sections through the first (B), second (C), third (D), and fourth (E) proboscis regions; F–I, cLSM micrographs of the proboscis labelled with phalloidin, F, z-projection of longitudinal sections of the anterior proboscis showing ICM, DM, and LM; G, H, substacks of transverse sections through the anterior proboscis showing muscle crosses (arrows); I, substacks of transverse sections through the middle proboscis (with DAPI). Abbreviations: ap, anterior proboscis; icm, inner circular musculature; mp, middle proboscis; ocm, outer circular musculature; pp, posterior proboscis. Scale bars: A = 100 μ m; B–G, I = 50 μ m; H = 20 μ m.

Beihai (21°29'41"N, 109°07'53"E), intertidal, muddy sand, collected by S. Sun; paratype (MIMB 41342), collected along with holotype.

Other material examined: 14 specimens (Ocean University of China), collected along with holotype.

Description: External appearance of live specimens. Live worms 14–18 mm long and 0.5–0.8 mm wide. Body cylindrical in foregut region, slightly flattened in its posterior half. Head rounded, narrower than the following body region, flattened dorso-ventrally (Fig. 6A–D), with white rhynchodaeum visible through integument (Fig. 6B, D, F). Mouth elongated (Fig. 6D, G). Cephalic furrows and ocelli absent. Body whitish, semitransparent (Fig. 6A), with gut region in some individuals yellowish brown. In nephridial region, body encircled with thin transverse ‘tubulanid ring’ (Fig. 6B–E); posterior to ring, epidermis opaque due to large number of glands (Fig. 6E); pair of poorly discernible oval lateral organs located in area of opaque epidermis (Fig. 6C).

Internal morphology: Body wall: in foregut region E 30–45 μm (up to 50 μm in precerebral region), D 1.5–2 μm , OCM 3–6 μm , LM 20–40 μm , ICM 4–6 μm . Immediately posterior to brain, epidermis with pair of latero-dorsal depressions (Fig. 7B). ICM not visible in transverse sections through posterior half of body. Longitudinal muscle plate between rhynchocoel and foregut present. Dorsal muscle crosses present between body-wall OCM and rhynchocoel circular musculature (Fig. 7E). Well-developed rhynchodaeal glandular epithelium forms four folds (Fig. 7A). Rhynchocoel extends for about 60% of body length; rhynchocoel wall consists of outer circular and inner longitudinal muscle layers, but longitudinal muscles reduced posteriorly of nephridial region (Fig. 7E). Proboscis has structure

similar to that of *Parahubrechtia rayi*, with short middle region (Fig. 6H); rod-shaped pseudocnidae 2.6–2.8 μm in length (Fig. 7F), occurring in clusters up to 100 pseudocnidae. Cephalic blood lacunae voluminous in squeezed live specimens (Fig. 6F), but very narrow in transverse sections (Fig. 7A). Lateral vessels run internal to ICM in foregut region (Fig. 7C), but in anterior intestine region lateral vessels pass through this layer and continue posteriorly between ICM and LM (Fig. 7D). Immediately anteriorly to mouth, two nerves arise from ventral part of ventral brain ganglia tightly adjoin each other without merging completely, then again diverge, forming two large buccal nerves. Large dorsal nerve single. Nephridial tubes with pair of narrow latero-dorsal openings and terminal glandular organ protruding into blood vessels laterally.

Ecology: The species inhabits the intertidal zone in muddy sand.

Distribution: South China Sea, Guanxi Province, Beihai.

Etymology: The specific name honors Prof. Per Sundberg, one of the authors of the genus *Parahubrechtia*.

Remarks: *Parahubrechtia peri* sp. nov. is distinguished from the two known species of *Parahubrechtia*, *P. jillae* Gibson and Sundberg, 1999 and *P. kvisti* Chernyshev, 2016, by a greater body length (*P. jillae* is 6–10 mm long, *P. kvisti* is 10–12 mm long), the developed inner longitudinal musculature of rhynchocoel in the foregut region (in *P. jillae* and *P. kvisti* isolated longitudinal muscle fibers do not form a definite layer), and thicker longitudinal muscle plate between rhynchocoel and foregut. In addition, from *P. jillae*, the new species differs by well-developed rhynchodaeal glandular epithelium. From *P. rayi*, the new species differs by a narrower head, which has a

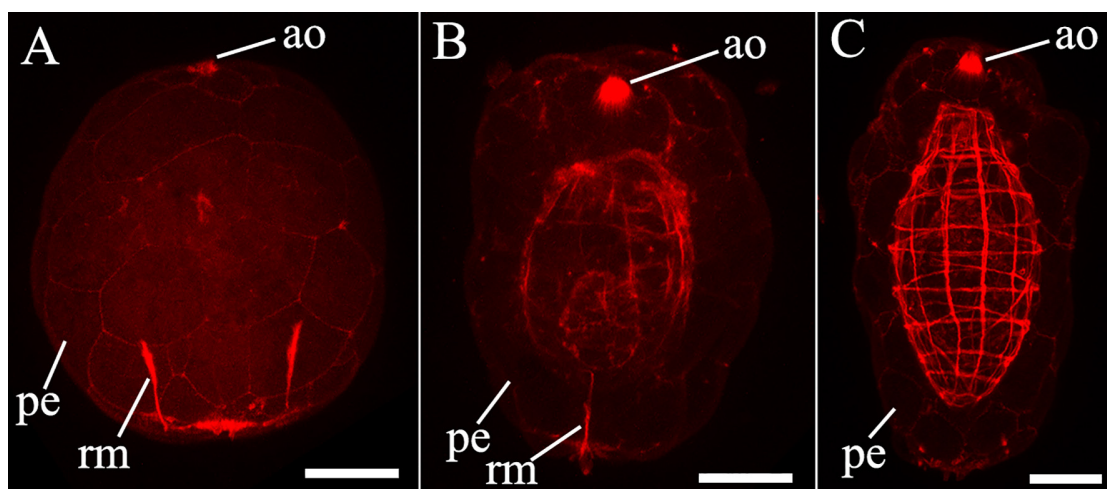


Fig. 5. *Parahubrechtia rayi* sp. nov., cLSM z-projections of the larvae labelled with phalloidin. A, stage at 26 h after fertilization; B, at 48 h after fertilization; C, at 72 h after fertilization. Abbreviations: ao, apical organ; pe, provisional epithelium; rm, retractor muscle. Scale bar = 20 μm .

pair of depressions, and by a thinner epidermis. The uncorrected *p*-distances between the *COI* of the *P. peri*, *P. rayi* and *P. kvisti* are 14.6–15.2% and 15.6–15.8%, respectively.

Phylogenetic analysis

The phylogenetic tree inferred from the analysis of concatenated dataset of five nuclear and mitochondrial

gene markers is relatively well resolved. The tree topology generated by Bayesian inference (BI) (Fig. 8) is largely congruent with the maximum likelihood (ML) analysis. The family Tubulanidae is highly supported (PP = 1, BP = 100). *Parahubrechtia rayi* and *P. peri* belong to the Tubulanidae, and together with *P. kvisti* form a highly supported subclade which is sister to *Callinera grandis* Bergendal, 1903. Three *Parahubrechtia* and four *Callinera* species, and also *Tubulanus pellucidus*



Fig. 6. *Parahubrechtia peri* sp. nov., live holotype (MIMB 41341). A, a relaxed specimen; B–D, anterior body portion of a relaxed specimen in the dorsal (B), lateral (C), and ventral (D) views (arrows indicate ‘tubulanid’ ring); E–H, a specimen compressed under coverglass with the anterior body half (E), precerebral region (F), mouth region (G), and a fragment of proboscis (H). Abbreviations: ap, anterior proboscis; br, brain; cl, cephalic lacuna; lo, lateral organ; mp, middle proboscis; pp, posterior proboscis; pr, proboscis; rd, rhynchodaeum; tr, ‘tubulanid’ ring. Scale bars: A = 2 mm; B–E = 0.5 mm; F–H = 0.1 mm.

(Coe, 1895) and Tubulanidae sp. California form a highly supported subclade within clade which also includes *Carinina plecta* Kajihara, 2006, two deep-sea Tubulanidae, and six *Tubulanus* species (*T. punctatus* (Takakura, 1898), *T. sexlineatus* (Griffin, 1898), *T. tamas* Kajihara, Kakui, Yamasaki and Hiruta, 2015, *T. riceae* Ritger and Norenburg, 2006, *T. rhabdotus* Corrêa, 1954, and *Tubulanus* sp. B Sakhalin). *Tubulanus annulatus* (Montagu, 1804), *T. polymorphus* Renier, 1804, *T. izuensis* Hookabe, Asai, Nakano, Kimura and Kajihara, 2020, *T. ezoensis* Yamaoka, 1940, and some unidentified Tubulanidae belong to another highly supported clade.

DISCUSSION

A recent phylogenetic analysis of the class Palaeonemertea (Chernyshev et al. 2021) supports distinction of five families: Carinomidae, Carininidae, Cephalotrichidae, Cephalotrichellidae, and Tubulanidae. The status of the family Carinomellidae remains

unclear, as no sequences have been obtained to date for its only species, *Carinomella lactea* Coe, 1905. However, the internal morphology of *C. lactea*, as well as the ultrastructure of its pseudocnidae, indicate its proximity to Tubulanidae (Chernyshev 1999; Magarlamov et al. 2021). Our phylogenetic analysis does not support the erection of the family Callineridae, since the genus *Callinera* along with species of the genus *Parahubrechtia* form a subclade within the clade Tubulanidae. Thus, the family Callineridae is a junior synonym to the family Tubulanidae, which was previously accepted by many authors (see Hylbom 1957). The close relationship of *Callinera* and *Parahubrechtia* unambiguously indicates that the latter genus belongs to the family Tubulanidae, rather than to Hubrechtidae, as was suggested previously (Sundberg and Hylbom 1994; Gibson and Sundberg 1999). These conclusions are confirmed by other phylogenetic analyses of paleonemerteans (Kvist et al. 2015; Chernyshev and Polyakova 2019; Hookabe et al. 2020).

Species of the genus *Parahubrechtia*, besides the type species, *P. jillae*, for which no sequences have

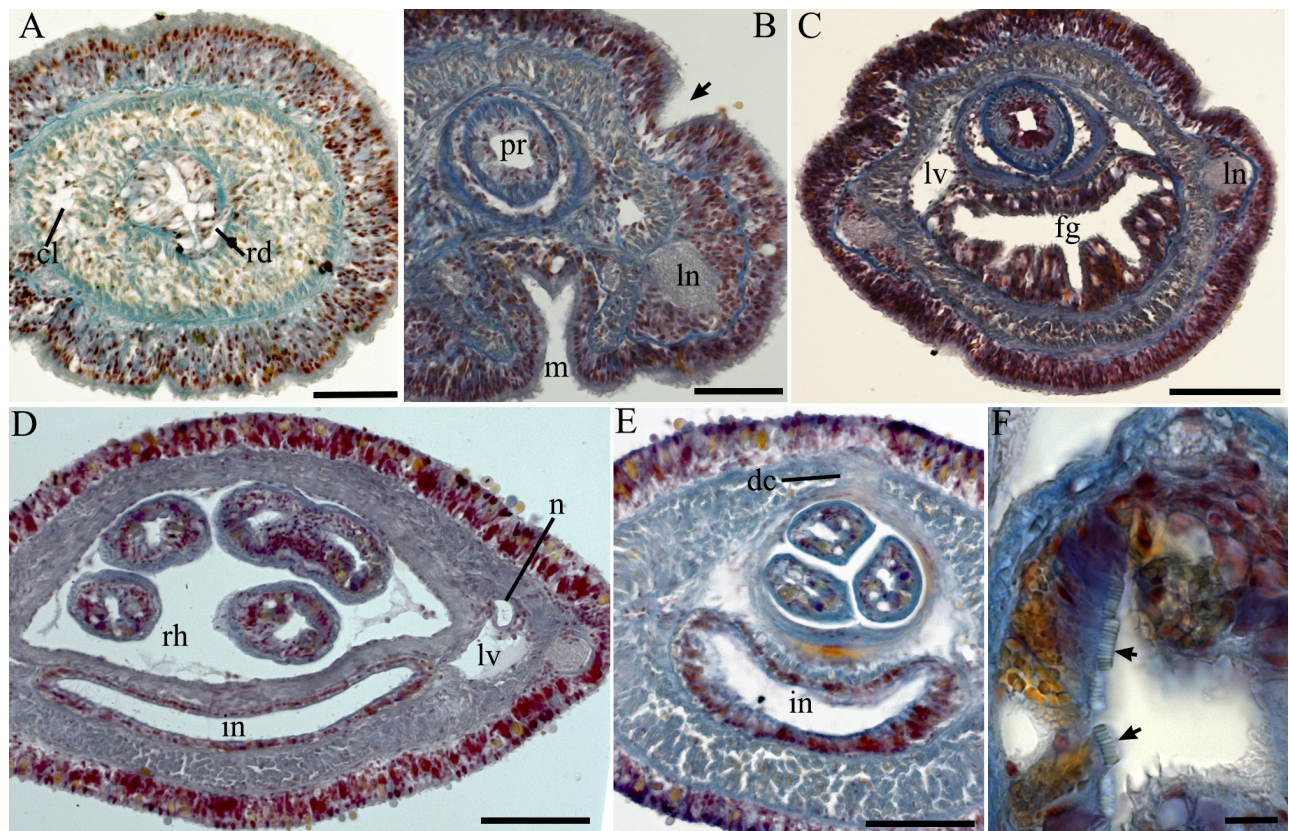


Fig. 7. *Parahubrechtia peri* sp. nov., transverse histological sections of the holotype. A, precerebral region; B, mouth region (arrow indicate epidermal depression); C, foregut region; D, nephridial region; E, post-nephridial region; F, anterior proboscis (arrows indicate pseudocnidae). Abbreviations: cl, cephalic lacuna; dc, dorsal muscle cross; fg, foregut; in, intestine; ln, longitudinal nerve cord; lv, lateral vessel; m, mouth; n, nephridial tube; pr, proboscis; rd, rhynchodaeum; rh, rhynchocoel. Scale bars: A, B = 50 μm; C–E = 100 μm; F = 10 μm.

been obtained, form a highly supported subclade. This deserves special attention, since no morphological synapomorphies have been identified for the genus *Parahubrechtia*. The genus *Parahubrechtia* comprises species lacking cerebral organs and with lateral organs, which have a simple proboscis and rhynchocoel morphology. The *Callinera* species also lack cerebral organs and have a pair of lateral organs (except for *C. grandis* and *C. monensis* Rogers et al., 1992), but their rhynchocoel is equipped with a posterior muscular sac, which is considered a synapomorphy of this genus. Apparently, most *Callinera* (excluding *C. emiliae* Kajihara, 2007) have a modified middle portion of the proboscis with special armament, which is a unique formation unknown for other palaeonemertean (see

Kajihara 2006; Chernyshev 2015).

Our phylogenetic analysis showed a close relationship between *Callinera* and *Parahubrechtia*, but did not confirm the monophyly of *Callinera*. The subclade *Callinera* + *Parahubrechtia* (tubulanids that are more closely related to *Parahubrechtia rayi* sp. nov. than to *T. polymorphus* Renier, 1804) includes two species from the coastal waters of the United States: Tubulanidae sp. from California and *Tubulanus pellucidus* from North Carolina. By external traits, *Tubulanus pellucidus* is almost indistinguishable from the *Parahubrechtia* species, but has transverse cephalic grooves and the associated cerebral organs. The specimen of *T. pellucidus* (MCZ 105594, GenBank), whose sequences were used in the phylogenetic

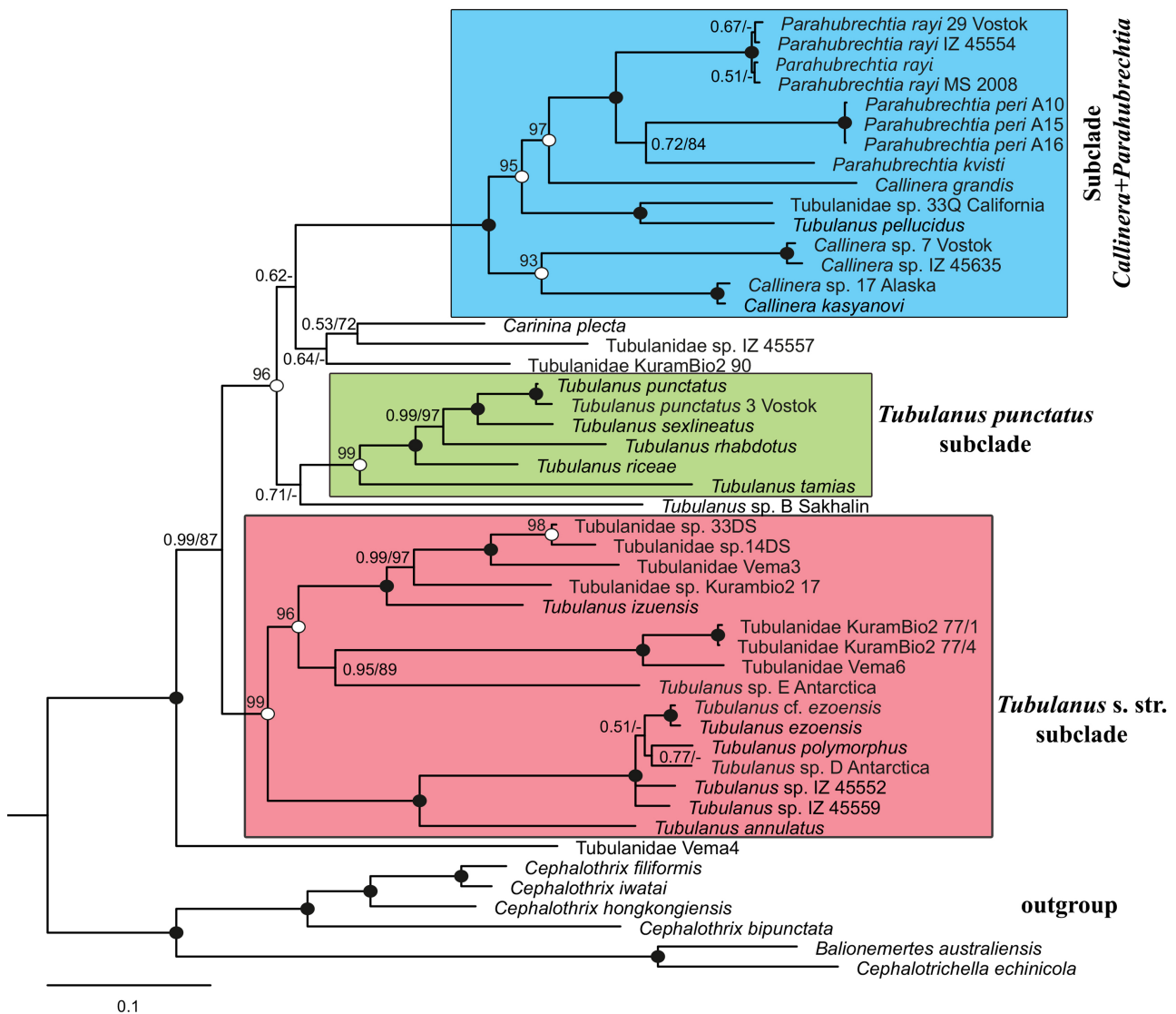


Fig. 8. Bayesian inference multilocus cladogram of Tubulanidae. Numerals near the branches are nodal support values (ML bootstrap value/Bayesian posterior probability). Closed circles indicate a nodal support of 1.00/100; open circles indicate a nodal support of 1.00/<100.

analysis, was identified without examination of its internal structure (James M. Turbeville, pers. inf.), and we suggest that it actually belongs to the genus *Parahubrechtia* or *Callinera*. If this suggestion is confirmed, a conclusion can be drawn that the subclade *Parahubrechtia* + *Callinera* has at least one synapomorphy, loss of cerebral organs. If paraphyly of *Callinera* is confirmed, the posterior rhynchocoel muscular sac, lost in the *Parahubrechtia* species, will also be a synapomorphy of the subclade *Parahubrechtia* + *Callinera*.

For making a decision whether *Parahubrechtia* is an independent genus or should be combined with *Callinera*, it is necessary to include other *Callinera* species in the phylogenetic analysis. The isolated position of *Callinera grandis* should be tested on additional material, since we did not use the sequence 28S (HQ856881) of this species from GenBank in the analysis, because it belongs to *Malacobdella grossa* (Müller, 1776). In addition, the analysis does not include representatives of the genera *Carinesta* or *Carinomella*, which also lack cerebral organs.

The paraphyly of the genus *Tubulanus*, whose representatives form two subclades, the subclade *Tubulanus* s. str. (tubulanids that are more closely related to *T. polymorphus* Renier, 1804 than to *T. punctatus* (Takakura, 1898)) and the subclade *Tubulanus punctatus* (tubulanids that are more closely related to *T. punctatus* than to *T. polymorphus*), should also be taken into account. In a further taxonomic revision of the Tubulanidae, the following solutions are possible: (1) splitting *Tubulanus* s.l. into two genera corresponding to the subclades *Tubulanus* s. str. and *Tubulanus punctatus*; these two genera will not include basal Tubulanidae Vema4, species of the subclade *Parahubrechtia* + *Callinera*, *Carinina plecta* (this species should be removed from the genus *Carinina* Hubrecht, 1885, see Chernyshev et al. 2021), *Tubulanus* sp. B Sakhalin, Tubulanidae sp. IZ 45557, and Tubulanidae KuramBio2 90; (2) combining all Tubulanidae into a single large genus, *Tubulanus* s.l., comprising *Parahubrechtia* and *Callinera*. The choice of one of the two solutions will depend on the results of a phylogenetic analysis of Tubulanidae involving a larger number of species.

CONCLUSIONS

The family Tubulanidae is a taxonomically challenging group, since many species lack the specific color pattern and differ only in characters of internal morphology. For this reason, the use of the so-called histological-free description approach for new species

is impossible. In the present report, we describe two new species from the genus *Parahubrechtia* which are very similar in external characters and internal morphology, but are well distinguished genetically. Even though our phylogenetic analysis includes significantly more species than previous analyses, we still cannot unambiguously decide whether the genus *Parahubrechtia* is independent or should be considered a junior synonym of *Callinera*. To address this issue, a more extensive phylogenetic analysis is required to include other species of the genus *Callinera*. Until such analysis, *Parahubrechtia* should be considered as a valid genus, endemic to the Pacific coast of Asia.

Acknowledgments: This work was supported by grant of the Ministry of Science and Higher Education, Russian Federation 13.1902.21.0012 ‘Fundamental Problems of Study and Conservation of Deep-Sea Ecosystems in Potentially Ore-Bearing Areas of the North-western Pacific’. Sun Shichun was supported by the National Natural Science Foundation of China (31471957). We thank Prof. Jon L. Norenburg and Dr. Herman Wirshing for assisting NEP with molecular work in the Smithsonian National Museum of Natural History; Prof. Jon L. Norenburg, Dr. Vladimir V. Mordukhovich, Olga V. Bozhenova, and Vasiliy G. Kuznetsov for providing the material. The authors are grateful to Miss Jia-Xuan Zhou for help in sequencing specimens of *Parahubrechtia peri* sp. nov. We are also grateful to Evgeniy P. Shvetsov for proofreading the English of this manuscript.

Authors’ contributions: AVC collected *Parahubrechtia rayi*, conducted the morphological examination, designed the present study and drafted the manuscript. NEP analysed molecular data and executed the phylogenetic analyses. SS collected and sequenced *Parahubrechtia peri*. All authors contributed to drafting and revising the manuscript. All authors read and approved the final manuscript.

Competing interests: The authors declare that they have no conflict of interests.

Availability of data and materials: The manuscript is incorporated in ZooBank. Type materials are deposited in the collections of MIMB. Sequences are deposited in GenBank.

Consent for publication: Not applicable.

Ethics approval consent to participate: Not applicable.

REFERENCES

- Andrade SCS, Strand M, Schwartz M, Chen H-X, Kajihara H, von Döhren J, Sun S, Junoy J, Thiel M, Norenburg JL, Turbeville JM, Giribet G, Sundberg P. 2012. Disentangling ribbon worm relationships: multi-locus analysis supports traditional classification of the phylum Nemertea. *Cladistics* **28**:141–159. doi:10.1111/j.1096-0031.2011.00376.x.
- Bergendal D. 1900. Till kännedom om de nordiska Nemertinerna. Öfversigt af Kongliga Vetenskaps-Akademiens Förhandlingar **57**:581–602.
- Bergendal D. 1902. Zur Kenntnis der nordischen Nemertinen. 2. Eine der construierten Urnemertine entsprechende Palaeonemerine aus dem Meere der schwedischen Westküste. *Zool Anz* **25**:421–432.
- Bergendal D. 1903. Till kännedom om de nordiska Nemertinerna. 4. Förteckning öfver vid Sveriges vestkust iakttagna Nemertiner. *Arkiv för Zoologi* **1**:85–156.
- Bürger O. 1892. Zur Systematik der Nemertinenfauna des Golfs von Neapel. Nachrichten von der Königlichen Gesellschaft der Wissenschaften und der Georg-Augusts-Universität zu Göttingen **5**:137–178.
- Bürger O. 1904. Nemertini. *Tierreich* **20**:1–151.
- Castresana J. 2000. Selection of conserved blocks from multiple alignments for their use in phylogenetic analysis. *Mol Biol Evol* **17**:540–552. doi:10.1093/oxfordjournals.molbev.a026334.
- Chernyshev AV. 1999. Nemertines of the family Carinomidae (Nemertea, Anopla). 2. Origin and taxonomic position of Carinomidae. *Zool Zh* **78**:1407–1416. (in Russian with English abstract)
- Chernyshev AV. 2002. A new nemertean, *Callinera zhirmunskiyi* sp. n., from the Pacific coast of Canada with a special reference to Callineridae taxonomy. *Russ J Mar Biol* **28**:132–135.
- Chernyshev AV. 2011. Comparative morphology, systematics and phylogeny of the nemerteans. *Dalnauka: Vladivostok*. (in Russian)
- Chernyshev AV. 2015. CLSM analysis of the phalloidin-stained muscle system of the nemertean proboscis and rhynchocoel. *Zool Sci* **32**:547–560. doi:10.2108/zs140267.
- Chernyshev AV. 2016. Nemerteans of the coastal waters of Vietnam. In: A.V. Adrianov and K.A. Lutaenko (eds) Biodiversity of the Western Part of the South China Sea. *Dalnauka, Vladivostok*.
- Chernyshev AV. 2021. An updated classification of the phylum Nemertea. *Invertebr Zool* **18**(3):188–196. doi:10.15298/invertzool.18.3.01.
- Chernyshev AV, Polyakova NE. 2018a. Nemerteans from deep-sea expedition SokhoBiol. with description of *Uniporus alisae* sp. nov. (Hoplonemertea: Reptantia s.l.) from the Sea of Okhotsk. *Deep Sea Res. Part II Top. Stud Oceanogr* **154**:121–139. doi:10.1016/j.dsr2.2017.09.022.
- Chernyshev AV, Polyakova NE. 2018b. Nemerteans of the Vema-TRANSIT expedition: First data on diversity with description of two new genera and species. *Deep Sea Res. Part II Top Stud Oceanogr* **148**:64–73. doi:10.1016/j.dsr2.2017.06.004.
- Chernyshev AV, Polyakova NE. 2019. Nemerteans from the deep-sea expedition KuramBio II with descriptions of three new hoplonemerteans from the Kuril-Kamchatka Trench. *Prog Oceanogr* **178**:102148. doi:10.1016/j.pocan.2019.102148.
- Chernyshev AV, Polyakova NE, Britayev TA, Bratova O, Mekhova ES. 2019. *Cephalotrichella echinicola* sp. nov. (Palaeonemertea, Cephalotrichellidae), a new nemertean associated with sea urchins from Nha Trang Bay (South China Sea). *Invertebr Syst* **33**:518–529. doi:10.1071/IS18080.
- Chernyshev AV, Polyakova NE, Hiebert TC, Maslakova SA. 2021. Evaluation of the taxonomic position of the genus *Carinina* (Nemertea: Palaeonemertea), with descriptions of two new species. *Invertebr Syst* **35**:245–260. doi:10.1071/IS20061.
- Coe WR. 1895. Descriptions of three new species of New England palaeonemerteans. *Trans Conn Acad Arts Sci* **9**:515–522.
- Coe WR. 1905. Nemerteans of the west and northwest coasts of America. *Bull Mus Compar Zool Harvard College* **47**:1–318.
- Colgan DJ, McLauchlan A, Wilson GDF, Livingston SP, Edgecombe GD, Macaranas J, Cassis G, Gray MR. 1998. Histone H3 and U2 snRNA DNA sequences and arthropod molecular evolution. *Austral J Zool* **46**:419–437. doi:10.1071/ZO98048.
- Corrêa DD. 1954. Nemertinos do litoral Brasileiro. *Bol Fac Filos Cienc Univ S Paulo* **19**:1–122.
- Folmer O, Black M, Hoch W, Lutz R, Vrijenhoek RC. 1994. DNA primers for amplification of mitochondrial cytochrome *c* oxidase subunit I from diverse metazoan invertebrates. *Mol Mar Biol Biotechnol* **3**:294–299.
- Gibson R. 1995. Nemertean genera and species of the world: an annotated checklist of original names and description citations, synonyms, current taxonomic status, habitats and recorded zoogeographic distribution. *J Nat Hist* **29**:271–562.
- Gibson R, Sundberg P. 1999. Six new species of palaeonemerteans (Nemertea) from Hong Kong. *Zool J Linn Soc* **125**:151–196. doi:10.1006/zjls.1997.0147.
- Giribet G, Carranza S, Baguna J, Riutort M, Ribera C. 1996. First molecular evidence for the existence of a Tardigrada + Arthropoda clade. *Mol Biol Evol* **13**:76–84. doi:10.1093/oxfordjournals.molbev.a025573.
- Griffin BB. 1898. Description of some marine nemerteans of Puget Sound and Alaska. *Ann NY Acad Sci* **11**:193–217.
- Hookabe N, Asai M, Nakano H, Kimura T, Kajihara H. 2020. A new bathyal tubulanid nemertean, *Tubulanus izuensis* sp. nov. (Nemertea: Palaeonemertea), from Japanese waters. *Proc Biol Soc Wash* **133**:122–133. doi:10.2988/PBSW-D-20-00006.
- Hubrecht AAW. 1879. The genera of European nemerteans critically revised, with description of several new species. *Note Leyden Mus* **1**:193–232.
- Hubrecht AAW. 1885. The Nemertea. *Narrativ of the Cruise of H.M.S. Challenger Expedition* **1**:830–833.
- Hylbom R. 1957. Studies on palaeonemerteans of the Gullmar Fiord area (west coast of Sweden). *Ark Zool, Ser 2* **10**:539–582.
- Iwata F. 1952. Nemertini from the coasts of Kyusyu. *J Fac Sci Hokkaido Univ Ser 6 Zool* **11**:126–148.
- Iwata F. 1957. Nemerteans from Sagami Bay. *Publ Akkeshi Mar Biol Stat* **7**:1–31.
- Kajihara H. 2006. Four palaeonemerteans (Nemertea: Anopla) from a tidal flat in middle Honshu, Japan. *Zootaxa* **1163**:1–47. doi:10.11646/zootaxa.1163.1.1.
- Kajihara H. 2007. *Callinera emiliae* sp. nov. (Nemertea: Palaeonemertea) from Negros Island, the Philippines. *Zootaxa* **1454**:39–47. doi:10.11646/zootaxa.1454.1.3.
- Kajihara H, Chernyshev AV, Sun S, Sundberg P, Crandall FB. 2008. Checklist of nemertean genera and species (Nemertea) published between 1995 and 2007. *Species Divers* **13**:245–274. doi:10.12782/specdiv.13.245.
- Kajihara H, Kakui K, Yamasaki H, Hiruta SF. 2015. *Tubulanus tamias* sp. nov. (Nemertea: Palaeonemertea) with two different types of epidermal eyes. *Zool Sci* **32**:596–604. doi:10.2108/zs140250.
- Katoh K, Standley DM. 2013. MAFFT multiple sequence alignment software version 7: improvements in performance and usability. *Mol Biol Evol* **30**:772–780. doi:10.1093/molbev/mst010.
- Kvist S, Laumer CE, Junoy J, Giribet G. 2014. New insights into the phylogeny, systematics and DNA barcoding of Nemertea. *Invertebr Syst* **28**:287–308. doi:10.1071/IS13061.

- Kvist S, Chernyshev AV, Giribet G. 2015. Phylogeny of Nemertea with special interest in the placement of diversity from Far East Russia and northeast Asia. *Hydrobiologia* **760**(1):105–119. doi:10.1007/s10750-015-2310-5.
- Lanfear R, Calcott B, Ho SYW, Guindon S. 2012. PartitionFinder: combined selection of partitioning schemes and substitution models for phylogenetic analyses. *Mol Biol Evol* **29**:1695–1701. doi:10.1093/molbev/mss020.
- Lanfear R, Calcott B, Kainer D, Mayer C, Stamatakis A. 2014. Selecting optimal partitioning schemes for phylogenomic datasets. *BMC Evol Biol* **14**:1–14. doi:10.1186/1471-2148-14-82.
- Littlewood DTJ. 1994. Molecular phylogenetics of cupped oysters based on partial 28S rRNA gene sequences. *Mol Phylogenet Evol* **3**:221–229. doi:10.1006/mpev.1994.1024.
- Magarlamov TYu, Turbeville JM, Chernyshev AV. 2021. Pseudocnidae of ribbon worms (Nemertea): ultrastructure, maturation, and functional morphology. *PeerJ* **9**:e10912. doi:10.7717/peerj.10912.
- McIntosh WC. 1873–1874. A Monograph of the British Annelids Part I. The Nemerteans. Ray Society, London, pp. 1–96, pls I–X in 1873; pp. 97–214, pls XI–XXIII in 1874.
- Minh BQ, Nguyen MAT, von Haeseler A. 2013. Ultrafast approximation for phylogenetic bootstrap. *Mol Biol Evol* **30**:1188–1195. doi:10.1093/molbev/mst024.
- Montagu G. 1804. Description of several marine animals found on the south coast of Devonshire. *Trans Linn Soc Lond* **7**:61–85.
- Müller OF. 1776. *Zoologiae danicae prodromus, seu animalium Daniae et Norvegiae indigenarum characteres, nomina, et synonyma imprimis popularium*. Havniae. Typis Hallageriis.
- Nguyen L-T, Schmidt HA, von Haeseler A, Minh BQ. 2015. IQ-TREE: A fast and effective stochastic algorithm for estimating maximum likelihood phylogenies. *Mol Biol Evol* **32**:268–274. doi:10.1093/molbev/msu300.
- Noren M, Jondelius U. 1999. Phylogeny of the Prolethophora (Platyhelminthes) Inferred from 18S rDNA Sequences. *Cladistics* **15**:103–112. doi:10.1111/j.1096-0031.1999.tb00252.x.
- Norenburg J, Gibson R, Herrera BA, Strand M. 2022. Callineridae Bergendal, 1901. In: World Nemertea Database. Available at: <http://www.marinespecies.org/nemertea/aphia.php?p=taxdetails&id=1451610>. Accessed 15 May 2022.
- Oersted AS. 1843. Forsog til en ny classification af Planarierne (Planariae Duges) grundet paa mikroskopisk-anatomiske Undersogelser. *Naturhistorisk Tidsskrift* **4**:519–581.
- Palumbi S, Martin A, Romano S, McMillan WO, Stice L, Grabowski G. 1991. The simple fools guide to PCR, ver. 2.0. Honolulu: Department of Zoology and Kewalo Marine Laboratory, University of Hawaii, USA.
- Punnett RC. 1900. On some South Pacific nemertines collected by Dr. Willey. *Zoological Results Based on Material from New Britain, New Guinea, Loyalty Islands and elsewhere, Collected during the years 1895, 1896 and 1897 by Arthur Willey, Part 5*:569–584.
- Renier SA. 1804. *Prospetto della Classe dei Vermi*. Padua, pp. xv–xxvii.
- Ritger RK, Norenburg JL. 2006. *Tubulanus riceae* new species (Nemertea: Anopla: Palaeonemertea: Tubulanidae), from South Florida, Belize and Panama. *J Nat Hist* **40**:931–942. doi:10.1080/00222930600833867.
- Rogers AD, Gibson R, Thorpe JP. 1992. A new species of *Callinera* (Nemertea, Anopla, Palaeonemertea) from the Isle of Man. *Zool Scr* **21**:119–128. doi:10.1111/j.1463-6409.1992.tb00314.x.
- Ronquist F, Teslenko M, van der Mark P, Ayres DL, Darling A, Höhna S, Larget B, Liu L, Suchard MA, Huelsenbeck JP. 2012. MrBayes 3.2: efficient Bayesian phylogenetic inference and model choice across a large model space. *Syst Biol* **61**:539–542. doi:10.1093/sysbio/sys029.
- Sands CJ, Convey P, Linse K, McInnes SJ. 2008. Assessing meiofaunal variation among individuals utilising morphological and molecular approaches: an example using the Tardigrada. *BMC Ecology* **8**:7. doi:10.1186/1472-6785-8-7.
- Strand M, Norenburg J, Alfaya JE, Fernández-Álvarez FÁ, Andersson HS, Andrade SCS, Bartolomeaus T, Beckers P, Bigatti G, Cherneva I, Chernyshev A, Chung BM, von Döhren J, Giribet G, Gonzalez-Cueto J, Herrera-Bachiller A, Hiebert T, Hookabe N, Junoy J, Kajihara H, Krämer D, Kvist S, Magarlamov TYu, Maslakova S, Mendes CB, Okazaki R, Sagorny C, Schwartz M, Sun S-C, Sundberg P, Turbeville JM, Xu C-M. 2019. Nemertean taxonomy—implementing changes in the higher ranks, dismissing Anopla and Enopla. *Zool Scr* **48**:118–119. doi:10.1111/zsc.12317.
- Sundberg P, Hylbom R. 1994. Phylogeny of the nemertean subclass Palaeonemertea (Anopla, Nemertea). *Cladistics* **10**(4):347–402. doi:10.1111/j.1096-0031.1994.tb00185.x.
- Sundberg P, Gibson R, Olsson U. 2003. Phylogenetic analysis of a group of palaeonemerteans (Nemertea) including two new species from Queensland and the Great Barrier Reef, Australia. *Zool Scr* **32**:279–296. doi:10.1046/j.1463-6409.2002.00032.x.
- Sundberg P, Chernyshev AV, Kajihara H, Kanneby T, Strand M. 2009. Character-matrix based descriptions of two new nemertean (Nemertea) species. *Zool J Linn Soc* **157**(2):264–294. doi:10.1111/j.1096-3642.2008.00514.x.
- Takakura U. 1898. Misaki-kinbōsan-himomushirui-(Nemertine)-nobunrui [A classification of the nemerteans of the Misaki region]. *Zool Mag* **10**:116–120. (in Japanese)
- Thollesson M, Norenburg JL. 2003. Ribbon worm relationships: A phylogeny of the phylum Nemertea. *Proc R Soc Lond B* **270**:407–414. doi:10.1098/rspb.2002.2254.
- Vaidya G, Lohman DJ, Meier R. 2011. SequenceMatrix: concatenation software for the fast assembly of multi-gene datasets with character set and codon information. *Cladistics* **27**:171–180. doi:10.1111/j.1096-0031.2010.00329.x.
- Vilgalys R, Sun BL. 1994. Ancient and recent patterns of geographic speciation in the oyster mushroom *Pleurotus* revealed by phylogenetic analysis of ribosomal DNA sequences. *Proc Nat Acad Sci USA* **91**:4599–4603. doi:10.1073/pnas.91.10.4599.
- Whiting MF, Carpenter JM, Wheeler QD, Wheeler WC. 1997. The Strepsiptera problem: Phylogeny of the holometabolous insect orders inferred from 18S and 28S ribosomal DNA sequences and morphology. *Syst Biol* **46**:1–68. doi:10.1093/sysbio/46.1.1.
- Wijnhoff G. 1913. Die Gattung *Cephalothrix* und ihre Bedeutung für die Systematik der Nemertinen. II. Systematischer Teil. *Zool Jb Abt Syst Ökol Geogr Tiere* **34**:291–320.
- Yamaoka T. 1940. The fauna of Akkeshi Bay. IX. Nemertini. *J Fac Sci Hokkaido Imperial Univ, Ser 6 Zool* **7**:205–263.
- Yurchenko OV, Neznanova SYu, Chernyshev AV. 2021. A comparative morphological study of the testes, spermatogenesis, and spermatozoa in two nemertean species, *Callinera* sp. and *Parahubrechtia* sp. (Palaeonemertea, Tubulanidae). *Zool Anz* **294**:114–127. doi:10.1016/j.jcz.2021.08.005.